# Focusing the wavefield inside an unknown 1D medium: Beyond seismic interferometry

Filippo Broggini[1], Roel Snieder[1], and Kees Wapenaar[2]

## ABSTRACT

With seismic interferometry one can retrieve the response to a virtual source inside an unknown medium, if there is a receiver at the position of the virtual source. Using inverse scattering theory, we demonstrate that, for a 1D medium, the requirement of having an actual receiver inside the medium can be circumvented, going beyond seismic interferometry. In this case, the wavefield can be focused inside an unknown medium with independent variations in velocity and density using reflection data only.

## INTRODUCTION

There are different ways to reconstruct the wavefield excited by a hypothetical source in the interior of an unknown medium. First, with seismic interferometry (Weaver and Lobkis, 2001; Wapenaar et al., 2005; Curtis et al., 2006; Schuster, 2009) it is possible to retrieve the response to a virtual source inside the medium with a receiver at the position where the virtual source is to be created, assuming the medium is surrounded by uncorrelated sources. The medium parameters need not be known. Second, in this paper, we show that, with 1D inverse scattering theory (Chadan and Sabatier, 1989; Gladwell, 1993; Colton and Kress, 1998), the response to a virtual source inside the medium can be obtained from reflected waves recorded at one side of the medium. We demonstrate that, in 1D media, this is possible without knowing the medium parameters. This is fascinating because it allows one to obtain the same virtual source response as with seismic interferometry (including all multiples), but without the need to have a receiver at the virtual source location. An essential element of this approach is to build an incident wave that is designed to collapse onto a point inside the medium at a specified time. The reconstructed wavefield can

be used to illuminate the medium under a complicated overburden, and the extracted Green's function can be used for imaging.

In this paper, the term focusing (Rose, 2001, 2002b) refers to the technique of finding an incident wave that collapses to a spatial delta function $\delta(z - z_0)$ at the location $z_0$ and at a prescribed time $t_0$ (i.e., the wavefield is focused at $z_0$ at $t_0$). In a 1D medium, we deal with a one-sided problem when observations from only one side of the perturbation are available (e.g., due to the practical consideration that we can only record reflected waves); otherwise, we call it a two-sided problem when we have access to both sides of the medium and account for reflected and transmitted waves.

## WAVEFIELD FOCUSING

Figure 1 shows the velocity and density profiles of a 1D acoustic medium. Note that velocity and density vary independently in depth. We simulate a numerical scattering experiment where an impulsive source is placed at the position $z = 2.44$ km. The acoustic wave equation is $LG(z, z_{VS}, t) = -\delta(z - z_{VS}) \frac{d}{dt} \delta(t)$, with the differential operator $L \equiv \rho(z) \frac{d}{dz} (\rho(z)^{-1} \frac{d}{dz}) - c(z)^{-2} \frac{d^2}{dt^2}$. Here, $z_{VS} = 2.44$ km and the initial condition is $G(z, z_{VS}, t < 0) = 0$. The incident wavefield propagates toward the discontinuities in the model, interacts with them, and generates scattered waves. We use a time-space finite-difference code with absorbing boundary conditions to simulate the propagation of the 1D waves and to produce the numerical examples shown in this section. For computational purposes, the source function $-\delta(z - z_{VS}) \frac{d}{dt} \delta(t)$ is convolved with a band-limited wavelet $s(t)$. The computed wavefield shown in Figure 2 represents the causal Green's function of the system $G$ convolved with $s(t)$. Causality ensures that the wavefield is nonzero only in the region delimited by the first arrivals (i.e., the direct waves) and we refer to it as the "causal region."

Due to practical limitations in field experiments, we usually are not able to place a source inside the medium we want to probe. However, when there are receivers inside the medium, seismic interferometry allows us to determine the wavefield as if there was a source at the position of any of the receivers, e.g., at $z = 2.44$ km.

This technique allows one to reconstruct the wavefield that propagates between a virtual source and other receivers located inside the medium (Wapenaar et al., 2005). This technique yields a combination of the causal wavefield $G$ and its time-reversed version $G^a$ (i.e., anticausal). This is due to the fact that the reconstructed wavefield propagates between a receiver and a virtual source. Conceptually speaking, without a real (physical) source, one must have nonzero incident waves on a receiver to create waves that emanate from that receiver. The fundamental equation to reconstruct the Green's function is (Wapenaar and Fokkema, 2006)

$$G(z, z_{VS}, t) + G(z, z_{VS}, -t)$$
$$\propto \sum_{z'=z_{S1}, z_{S2}} G(z, z', t) * G(z_{VS}, z', -t), \quad (1)$$

where $z_{VS} = 2.44$ km, and $z_{S1}$ and $z_{S2}$ are the coordinates of impulsive sources located at both sides of the perturbation (a total of two sources in 1D) as shown at the bottom of Figure 1. Between $z_{S1}$ and $z_{S2}$, the causal part of the wavefield estimated by this
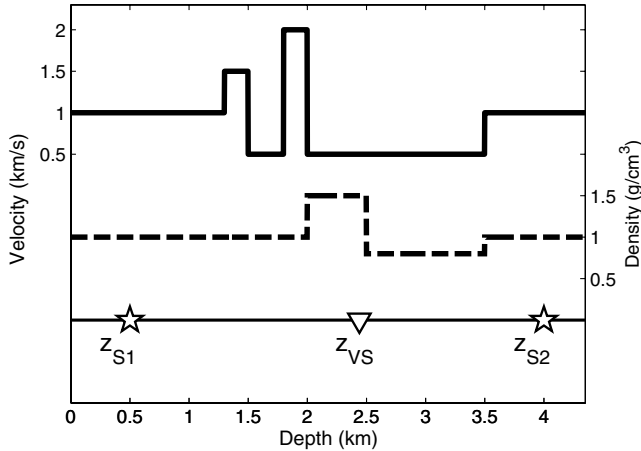


Figure 1. Top: Velocity profile of the 1D model (solid line). The perturbation in the velocity is located between $z = 1.3$–$3.5$ km and $c_0 = 1$ km/s. Middle: Density profile of the 1D model (dashed line). The perturbation in the density is located between $z = 2.0$–$3.5$ km and $\rho_0 = 1$ g/cm$^3$. Bottom: Locations of the real and virtual sources for seismic interferometry; $z_{S1}$ and $z_{S2}$ indicate the two real sources and $z_{VS}$ shows the virtual source location.
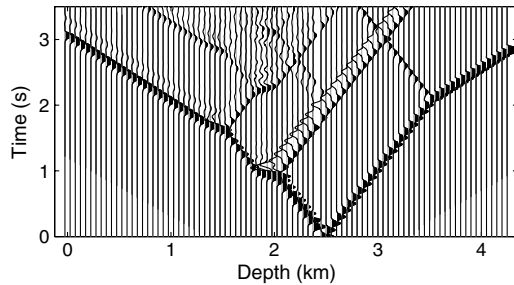


Figure 2. Response to a source located at $z = 2.44$ km. The traces are recorded by receivers located at each location in the model (shown in Figure 1) with a spacing of 40 m. Waves are emanating from the line $t = 0$ s only at $z = 2.44$ km.

Green's function reconstruction technique is consistent with the wavefield shown in Figure 2.

We thus have two different ways to obtain the same wavefield, but often we cannot place any sources or receivers inside the medium. We next assume that we only have access to reflected waves $R(t)$ measured above the perturbation, i.e., the reflected impulse response measured at $z = 0$ km due to an impulsive source placed at $z = 0$ km. This limitation raises another question: Can we reconstruct the same wavefield shown in Figure 2 having knowledge only of the reflected waves $R(t)$? For this 1D problem, the answer to this question is given by the Marchenko equation (Lamb, 1980; Chadan and Sabatier, 1989). Its solution provides a particular incident wave that collapses the wavefield to a spatial delta function at the desired location after it interacts with the medium, and this incident wave consists of a delta function added to the solution of the Marchenko equation (Rose, 2001, 2002a).

The Marchenko integral equation is a fundamental relation of 1D inverse scattering theory. It is an integral equation that relates the reflected waves $R(t)$ to the incident wavefield $u(t, t_f)$, which creates a focus in the interior of the medium and ultimately gives the perturbation of the medium. The 1D form of this equation is

$$0 = R(t + t_f) + u(t, t_f) + \int_{-\infty}^{t_f} R(t + t')u(t', t_f)dt', \quad (2)$$

where $t_f$ is the one-way traveltime from $z = 0$ to the focusing location. We numerically solve the Marchenko equation and construct the particular incident wave that focuses at $t = 0$ s at a location specified by $t_f = 3$ s. Any appropriate numerical method to solve integral equations can be used to compute $u(t, t_f)$ (e.g., an iterative method). Note that solving equation 2 does not require any knowledge of the medium: All that is needed is the reflection response $R(t)$ and the one-way traveltime $t_f$, which specifies the location of the focus. Next, we inject the particular incident wave $\delta(t + t_f) + u(-t, t_f)$ at $z = 0$ km and compute the time-space diagram shown in the top panel of Figure 3. This shows the wavefield when the incident wave is injected at $z = 0$ into the model. We define this wavefield as $K(z, t)$. The time-space diagram shown in Figure 3 is computed using the true model, but this is done only to illustrate the physics of the focusing process. The bottom panel of Figure 3 shows a cross section of the wavefield at time $t = 0$ s: The wavefield vanishes except at location $z = 2.44$ km. For this particular model, $t_f = 3$ s corresponds to spatial focusing at the same location where we placed the virtual source in Figure 1. We emphasize that this method is data driven, hence the true model is not needed to build the particular incident wavefield.

Figure 3 does not yet resemble the wavefield shown in Figure 2. In fact, in Figure 3 waves cross the solid line at $t = 0$ s for locations $z \leq 2.44$ km, whereas in Figure 2 waves cross the same solid line only at the virtual source location $z = 2.44$ km. However, denoting as $K(z, -t)$ the time-reversed version of $K(z, t)$, we obtain the wavefield shown in Figure 4 by adding $K(z, t)$ and $K(z, -t)$. With this summation, we create the response to a virtual source located at $z_{VS} = 2.44$ km, namely $G(z, z_{VS}, t) + G(z, z_{VS}, -t)$ (convolved with $s(t)$). This step is the main result of this paper. Note that the trace at $z = 0$, $K(0, t) + K(0, -t)$, has been obtained without any information about the model. As in Figure 3, the remainder of Figure 4 is based on the true model and is only shown to explain the physics of the focusing process. In Figure 4, the wavefield outside the causal region is zero because the portion of $K(z, t)$ outside

the causal region is antisymmetric in time and hence cancels in the sum $K(z, t) + K(z, -t)$. With this process, we effectively go from one-sided to two-sided illumination because in Figure 4 waves are incident onto the focusing location from both sides for $t < 0$ s. The incident waves are non zero for $-6$ s $< t < -3$ s, but to facilitate a comparison with Figure 2 this time interval is not completely included in the figure. According to Figure 4, we create a focus at a location inside the inhomogeneous medium without having a source or a receiver at such a location and without any knowledge of the medium properties; we only have access to the reflected impulse response measured above the perturbation. With an appropriate choice of sources and receivers, this experiment can be done in practice, e.g., in an acoustics laboratory (Rose, 2002a). Burridge (1980) shows diagrams similar to Figures 3 and 4 and explains how to combine such diagrams using causality and symmetry properties. The wavefield for positive times $t > 0$ (causal region) in Figure 4 corresponds to the causal Green's function $G$ and the wavefield for negative times $t < 0$ represents the anticausal Green's function $G^a$ (defining the anticausal region). A small amount of energy is outside of the causal and anticausal regions due to numerical inaccuracies in our solution of the Marchenko equation (this is also visible in the bottom panel of Figures 3 and 4). The causal part of the trace at $z = 0$ km is the virtual source response $G(0, z_{VS}, t)$ that we obtained without using the model.

The anticausal Green's function $G^a$ follows from $G$ by time-reversal, hence it satisfies $LG^a = -\delta(z - z_{VS})\frac{d}{d(-t)}\delta(-t) = \delta(z - z_{VS})\frac{d}{dt}\delta(t)$, where we used that $L$ is invariant to time-reversal. Adding the differential equations for $G$ and $G^a$ shows that $G + G^a$ satisfies the homogeneous equation: $L(G + G^a) = -\delta(z - z_{VS})\frac{d}{dt}\delta(t) + \delta(z - z_{VS})\frac{d}{dt}\delta(t) = 0$. The term "homogeneous" suggests that the sum of $G$ and $G^a$ is source-free. Hence, to focus the wavefield at the virtual source location, there must be a particular incident wavefield coming from another location. In fact, the knowledge that $G + G^a$ satisfies a homogeneous equation suggests that a combination of the causal and anticausal Green's functions is needed to focus the wavefield at a location where there is no real source (i.e., source-free), as shown in Figure 4. Oristaglio (1989) shows a similar result, although he derives the difference (instead of the sum) of the causal and anticausal Green's functions due to a different definition of the Green's functions.

## DISCUSSION

In the previous section, we use the one-way traveltime $t_f$ to determine the depth $z_{VS}$ of the virtual source. In other words, the wavefield focuses at the virtual source location $z_{VS}$ after it has propagated inside the medium for a length of time equal to $t_f$. To directly choose a prescribed focusing location $z_{VS}$ (and not a prescribed one-way traveltime $t_f$), we need to know the average velocity of the medium between the surface and the depth of the focusing location. However, no information about either the density or the details of the velocity profile is required.

This method also works when density and velocity vary independently. This fact is a new contribution because the previous inverse scattering theory of (Rose 2001, 2002b) and others (Aktosun and Rose, 2002) does not deal with simultaneous changes in density and velocity because one cannot retrieve two independent quantities from one time series of reflected waves. We also add another step beyond the work of Rose by forming the sum $K(z, t) + K(z, -t)$, which ensures that the wavefield vanishes outside the causal and anticausal regions and creates the response of the virtual source. We show that the interaction between causal and anticausal wavefields is a key element to focus the wavefield where there is no real source.

We are currently investigating the application of the central ideas of this work to wave propagation in two and three dimensions
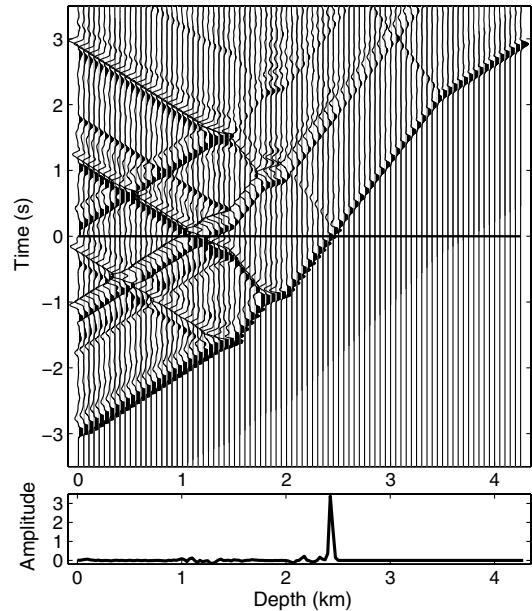


Figure 3. Top: At $z = 0$ km, we inject the particular incident wave in the model and compute the time-space diagram by forward modeling. We denote this wavefield as $K(z, t)$. Waves cross the solid line at $t = 0$ s for locations $z \leq 2.44$ km. Note that the waves continue to propagate after 3 s. Bottom: Cross section of the wavefield at $t = 0$ s.

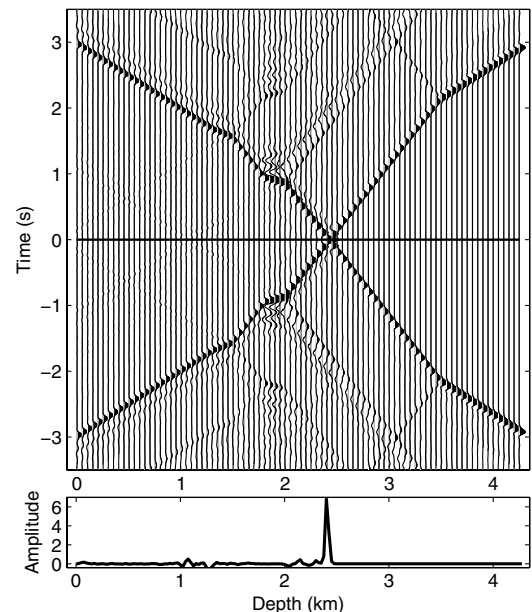

Figure 4. Top: Wavefield that focuses at $z = 2.44$ km at $t = 0$ s without a source or a receiver at this location. This wavefield corresponds to $K(z, t) + K(z, -t)$ and consists of a causal ($t > 0$) and an anticausal ($t < 0$) region. Bottom: Cross section of the wavefield at $t = 0$ s.

(Wapenaar et al., 2011). This extension allows us to focus the wavefield to a point in the subsurface to simulate a source at depth and to record data at the surface. This kind of application will be helpful for full-waveform inversion (Brenders and Pratt, 2007) and subsalt imaging (Sava and Biondi, 2004), where waves that have traversed a strongly inhomogeneous overburden are of extreme importance. We speculate that focusing the wavefield at a prescribed location in 2D and 3D media requires an estimate of the primary traveltimes from the virtual source location to the receivers (e.g., using a macro model). Wapenaar et al. (2012) give a first mathematical proof for a 2D medium with density variations only.

## CONCLUSIONS

There are three distinct ways to reconstruct the same physical wave state. A physical source, seismic interferometry, and inverse scattering theory allow one to create the same wave state that focuses at a certain location $z_{VS}$. Seismic interferometry tells us how to build an estimate of the wavefield without knowing the medium properties, if we have a receiver at the same location $z_{VS}$ of the real source in the scattering experiment of Figure 2 and sources surrounding the medium. Inverse scattering goes beyond this as it allows us to focus the wavefield inside the medium without knowing its properties, using only reflected waves $R(t)$ recorded at one side of the medium.

## ACKNOWLEDGMENTS

## REFERENCES

Aktosun, T., and J. H. Rose, 2002, Wave focusing on the line: Journal of Mathematical Physics, **43**, no. 7, 3717–3745, doi: 10.1063/1.1483894.

Brenders, A. J., and R. G. Pratt, 2007, Full-waveform tomography for lithospheric imaging: Results from a blind test in a realistic crustal model: Geophysical Journal International, **168**, 133–151, doi: 10.1111/gji.2007.168.issue-1.

Burridge, R., 1980, The Gelfand-Levitan, the Marchenko, and the Gopinath-Sondhi integral equations of inverse scattering theory, regarded in the context of inverse impulse-response problems: Wave Motion, **2**, 305–323, doi: 10.1016/0165-2125(80)90011-6.

Chadan, K., and P. C. Sabatier, 1989, Inverse problems in quantum scattering theory: 2nd ed., Springer.

Colton, D., and R. Kress, 1998, Inverse acoustic and electromagnetic scattering theory: Springer.

Curtis, A., P. Gerstoft, H. Sato, R. Snieder, and K. Wapenaar, 2006, Seismic interferometry–-turning noise into signal: The Leading Edge, **25**, 1082–1092, doi: 10.1190/1.2349814.

Gladwell, G. M. L., 1993, Inverse problems in scattering: Kluwer Academic Publishing.

Lamb, G. L., 1980, Elements of soliton theory: Wiley-Interscience.

Oristaglio, M., 1989, An inverse scattering formula that uses all the data: Inverse Problems, **5**, 1097–1105, doi: 10.1088/0266-5611/5/6/015.

Rose, J. H., 2001, "Single-sided" focusing of the time-dependent Schrödinger equation: Physical Review Abstracts, **65**, no. 1, 012707, doi: 10.1103/PhysRevA.65.012707.

Rose, J. H., 2002a, Single-sided autofocusing of sound in layered materials: Inverse Problems, **18**, 1923–1934, doi: 10.1088/0266-5611/18/6/329.

Rose, J. H., 2002b, Time reversal, focusing and exact inverse scattering, in imaging of complex media with acoustic and seismic waves: Springer, 97–106.

Sava, P., and B. Biondi, 2004, Wave-equation migration velocity analysis — Part II: Subsalt imaging example: Geophysical Prospecting, **52**, 607–623, doi: 10.1111/gpr.2004.52.issue-6.

Schuster, G. T., 2009, Seismic interferometry: Cambridge University Press.

Wapenaar, K., F. Broggini, and R. Snieder, 2011, A proposal for model-independent 3D wave field reconstruction from reflection data: 81st International Annual Meeting, SEG, Expanded Abstracts, 3788–3792.

Wapenaar, K., F. Broggini, and R. Snieder, 2012, Creating a virtual source inside a medium from reflection data: Heuristic derivation and stationary-phase analysis: Geophysical Journal International, **190**, no. 2, 1020–1024, doi: 10.1111/j.1365-246X.2012.05551.x.

Wapenaar, K., and J. Fokkema, 2006, Green's function representations for seismic interferometry: Geophysics, **71**, no. 4, SI33–SI46, doi: 10.1190/1.2213955.

Wapenaar, K., J. Fokkema, and R. Snieder, 2005, Retrieving the Green's function in an open system by cross correlation: A comparison of approaches (L): Journal of the Acoustical Society of America, **118**, 2783–2786, doi: 10.1121/1.2046847.

Weaver, R., and O. Lobkis, 2001, Ultrasonics without a source: Thermal fluctuation correlations at mhz frequencies: Physical Review Letters, **87**, no. 13, 134301, doi: 10.1103/PhysRevLett.87.134301.